

Dynamical Heterogeneity Close to the Jamming Transition in a Sheared Granular Material

O. Dauchot and G. Marty

SPEC, CEA-Saclay, 91 191 Gif-sur-Yvette, France

G. Biroli

SPhT, CEA-Saclay, 91 191 Gif-sur-Yvette, France

(Received 6 July 2005; published 27 December 2005)

The dynamics of a bidimensional dense granular packing under cyclic shear is experimentally investigated close to the jamming transition. Measurement of multipoint correlation functions are produced. The self-intermediate scattering function, displaying slower than exponential relaxation, suggests dynamic heterogeneity. Further analysis of four point correlation functions reveal that the grain relaxations are strongly correlated and spatially heterogeneous, especially at the time scale of the collective rearrangements. Finally, a dynamical correlation length is extracted from a spatiotemporal pattern of mobility. Our experimental results open the way to a systematic study of dynamic correlation functions in granular materials.

DOI: [10.1103/PhysRevLett.95.265701](https://doi.org/10.1103/PhysRevLett.95.265701)

PACS numbers: 64.70.Pf, 05.40.Ca, 45.70.Cc, 61.43.Fs

The dynamical behavior of granular media close to the “jamming transition” is very similar to that of liquids close to the glass transition [1]. Indeed, granular media close to jamming display a similar dramatic slowing down of the dynamics [2,3] as well as other glassy features such as aging and memory effect [4]. Recently, a “microscopic” confirmation of the above similarity has been obtained analyzing directly the grain dynamics under cyclic shear during compaction [5] or at constant density [6]. The typical trajectories of grains display the so-called cage effect and are remarkably similar to the ones observed in experiments on colloidal suspension [7] and in molecular dynamics simulations of glass formers [8]. As for glass formers, and contrary to standard critical slowing down, this slow glassy dynamics does not seem related to a growing *static* local order. For glass formers it has been shown numerically [9–12] and experimentally [13] that instead the *dynamics* becomes strongly heterogeneous and *dynamic correlations* build up when approaching the glass transition. The existence of a growing dynamic correlation length is very important to reveal some kind of criticality associated with the glass transition [14].

Here we also unveil that granular materials are strongly dynamically correlated close to the jamming transition. First, we shall focus on two point functions, in particular, the self-intermediate scattering function, whose slower than exponential relaxation suggests dynamic heterogeneity. Then, following recent theoretical suggestions [15,16], we shall turn to four point correlation functions. They have been introduced for glass formers to measure properly dynamic correlations [17] and indeed reveal that the dynamics is strongly correlated and heterogeneous. Finally, we shall focus on spatiotemporal pattern of mobility, out of which we extract a direct measurement of a dynamical length scale. Our experimental results, to our knowledge the first direct measurement of four point *spatiotemporal*

correlation functions [18], open the way to a systematic study of dynamic correlation functions in granular material as a way towards a better understanding of glassy and “jammy” materials in general. The experimental setup, a more robust and better designed version of the one presented in Ref. [6] is as follows: a bidimensional, bi-disperse granular material, composed of about 8.000 metallic cylinders of diameter 5 and 6 mm in equal proportions, is sheared quasistatically in an horizontal deformable parallelogram. The shear is periodic, with an amplitude $\theta_{\max} = \pm 5^\circ$. The volume fraction ($\Phi = 0.84$) is maintained constant by imposing the height of the parallelogram. We follow 2818 grains located in the center of the device to avoid boundary effects with a high resolution digital camera which takes a picture each time the system is back to its initial position $\theta = 0$. The unit of time is one cycle, a whole experiment lasting 10.000 cycles. The unit of length is chosen to be the mean particle diameter d . These conditions are very similar to Ref. [6] and by repeating the same analysis we find a cage radius of 0.2 and a cage lifetime of 300. As discussed in Ref. [6], the diffusion is isotropic, at least far from the borders of the experimental cell.

Let us first focus on the self-intermediate scattering function which measures the dynamics of single particles:

$$F_s = \langle \hat{F}_s(k, t) \rangle = \frac{1}{N} \sum_j \langle \exp[-ik(r_j(t) - r_j(0))] \rangle, \quad (1)$$

where $r_j(t)$ is the position of the j th particles at time t . $\hat{F}_s(k, t)$ denotes the nonaveraged instantaneous observable. $\langle \cdot \rangle$ means (here and in the following) a time average over 300 steps of 10 cycle each computed after a few thousand cycles, when the systems has reached a steady state (at least on the time scale of the experiment). The sum in (1) is over all tracked particles.

The function $F_s(k, t)$ is plotted on the left of Fig. 1 as a function of time for different odd values of k ranging from 1 to 29. Contrary to glass formers there is no visible plateau in this correlation function although from trajectories it is possible to identify a clear cage effect (see Fig. 2 of Ref. [6]). Note that the short-time dynamics is subdiffusive [6] probably because granular media do not experience thermal relaxation. Therefore the separation of time scales and the corresponding plateau in correlation functions is much less pronounced as in colloids [7]. Analyzing the curves in Fig. 1 we find that the decreasing of $F_s(k, t)$ is slower than exponential in time. A good fit is provided by a stretched exponential: $\exp[-(t/\tau(k))^{\beta(k)}]$. We plot on the right of Fig. 1 $\tau(k)$ (top) and $\beta(k)$ (bottom) as a function of k . At small k the relaxation time scales as k^{-2} and the exponent $\beta(k)$ is one. As expected, the grains perform a Brownian motion on large length and time scales and therefore $F_s(k, t) \approx \exp(-Dk^2t)$ for small k and large t . Increasing k the stretched exponent decreases and is of the order of 0.7 for k of the order of 2π , corresponding to the intergrain distance, and even lower for higher values of k . A very similar behavior has been found for glass formers [8,13]. Also the decrease of $\tau(k)$ steepens and decreases sharply for large k . This is also related to the short-time subdiffusive dynamics. In this regime the particle displacement distribution has a variance scaling as $t^{1/2}$ (not t like for standard diffusion) and is well fitted by a Gaussian. Assuming this functional form and Fourier transforming to get the intermediate scattering function, one finds that the relaxation time goes as k^{-4} , hence a crossover from a k^{-2} behavior at small k to a more rapid decreasing at large k as in Fig. 1.

Dynamical heterogeneity is one of the possible explanation of the nonexponential relaxation of $F_s(k, t)$: the relaxation becomes slower than exponential because there is a strong spatial distribution of time scales [13]. This

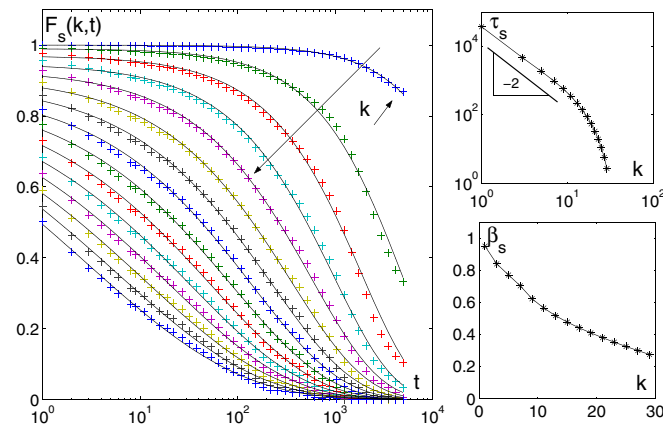


FIG. 1 (color online). On the left: $F_s(k, t)$ as a function of time for different odd values of the wave vector $k = 1, 3, \dots, 29$ from top to bottom (as indicated by the arrow and the increasing $k \nearrow$). The black lines are fits of the form $\exp[-(t/\tau(k))^{\beta(k)}]$. On the right: $\tau(k)$ (top) and $\beta(k)$ (bottom) as a function of k .

effect is strong for intermediate and large values of k . Instead for smaller k s, the heterogeneities are averaged out and a larger value of $\beta(k)$, going to one for $k \rightarrow 0$, is expected. This coincides indeed with the trend found in Fig. 1. However, this is not the only possible scenario [13,19]. In the following we want to go one step further and show direct “smoking gun” evidence of dynamical correlations. For this purpose it is of interest to consider the *structural relaxation* and not only the single particle one, as given by $F_s(k, t)$. We focus on the density overlap [17] following previous works on glass-forming liquids:

$$Q^a = \langle \hat{Q}^a \rangle = \frac{1}{N} \int dr dr' \langle \delta \rho(r, t) w_a(r - r') \delta \rho(r', 0) \rangle, \quad (2)$$

where $\rho(r, t) = \sum_i \delta(r - r_i(t))$ and $\delta \rho(r, t) = \rho(r, t) - \langle \rho \rangle$. The overlap function is a non-normalized Gaussian: $w_a(r) = \exp(-r^2/2a^2)$. The evolution of $Q^a(t)$ is a measure of how long it takes to the systems to decorrelate from its density profile at time $t = 0$. Figure 2 shows that the behavior of $Q^a(t)$ is similar to the one of $F_s(k, t)$, as for glass formers [11,17]. The proper way to unveil spatiotemporal correlations is through the fluctuations of the temporal relaxation [17]. Those are characterized by dynamical susceptibilities:

$$\chi_4^H(k, t) = N \langle (\hat{H}(k, t) - \langle \hat{H}(k, t) \rangle)^2 \rangle \quad (3)$$

where H can either be $F_s(k, t)$ or $Q^a(t)$. They unveil dynamic correlations exactly as fluctuations of the magnetization unveil magnetic correlations close to a ferromagnetic transition; see, e.g., Refs. [20,21]. One way to understand how such susceptibilities relate to spatial heterogeneities of the dynamics is to decompose, say, $\hat{Q}^a(t)$ in local contributions: $N \hat{Q}^a(t) = \rho \int dr \hat{q}^a(r, t)$ where $\hat{q}^a(r, t) = \frac{1}{\rho} \int dr' \delta \rho(r, t) w_a(r - r') \delta \rho(r', 0)$. Using this expression one finds $\chi_4^Q(t) = \rho \int dr G_4^Q(r, t)$ where $G_4^Q(r, t) = \langle [\hat{q}^a(r, t) - \langle \hat{q}^a(r, t) \rangle][\hat{q}^a(0, t) - \langle \hat{q}^a(0, t) \rangle] \rangle$ is the spatial correlation of the local temporal relaxation: if at point 0 an event has occurred that leads to a decorrela-

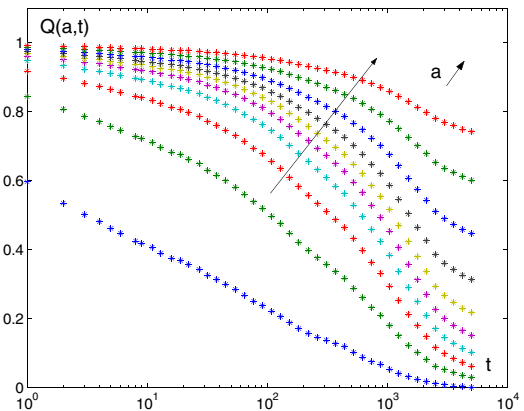


FIG. 2 (color online). $Q_a(t)$ as a function of time for $a = 0.05, 0.1, \dots, 0.5$.

tion of the local density over the time scale t , $G_4^Q(r, t)$ is the probability that a similar event has occurred a distance r away, within the same time interval t . $\chi_4^Q(t)$, its volume integral, quantifies how spatially correlated the dynamics is (see Refs. [9,11,20,21] for a more detailed discussion).

Figure 3(a) displays $\chi_4^{F_s}(t)$ for $k = 1, 3, \dots, 29$. It has the form found for glass formers [9,11,12,17,21]: it is of the order of 1 at small and large time and displays a peak at a time somewhat larger than the time scale of the subdiffusive regime. The peak is a clear signature of dynamic heterogeneity and shows that the dynamics is maximally correlated on time scales of the order of the relaxation time. A rough estimation of the corresponding dynamical correlation length is obtained identifying the peak of $\chi_4^{F_s}(t)$, of the order of 100, to a correlated area $\pi \xi_{\text{het}}^2$, leading to a length $\xi_{\text{het}} \propto 6$ in agreement with a previous estimate [6]. We find very similar results for $\chi_4^Q(t)$, as shown in Fig. 3(b) for $a = 0.05, 0.1, \dots, 0.5$. The largest $\chi_4^Q(t)$ is obtained for $a = 0.15$, which corresponds to the typical displacement during the subdiffusive regime. Large and small values of a corresponds to small values of the peak because the dynamics on small length scales is certainly not very correlated and on very long length scales the heterogeneous character of the dynamics is averaged out. As discussed in Ref. [21], the power law growth of $\chi_4^{F_s}(t)$

$[\chi_4^Q(t)]$ before the peak with exponents between 1 and 2/3 (see insets of Fig. 3) suggest that the dynamic correlations cannot be induced by independent defect or free volume diffusion.

We now focus on spatiotemporal patterns of mobility.

Figure 4 presents a gray-scale plot of $\hat{q}_s^a(r, t) = \sum_i \delta(r - r_i(0)) w_a(r_i(t) - r_i(0))$ for $t = 42, 435, 1113, 2526$, and $a = 0.15$, where $\delta(r)$ is approximated by a Gaussian of width 0.3. By definition $\hat{q}_s^a(r, t)$ measures a coarse grained mobility: if the particle that was close to r

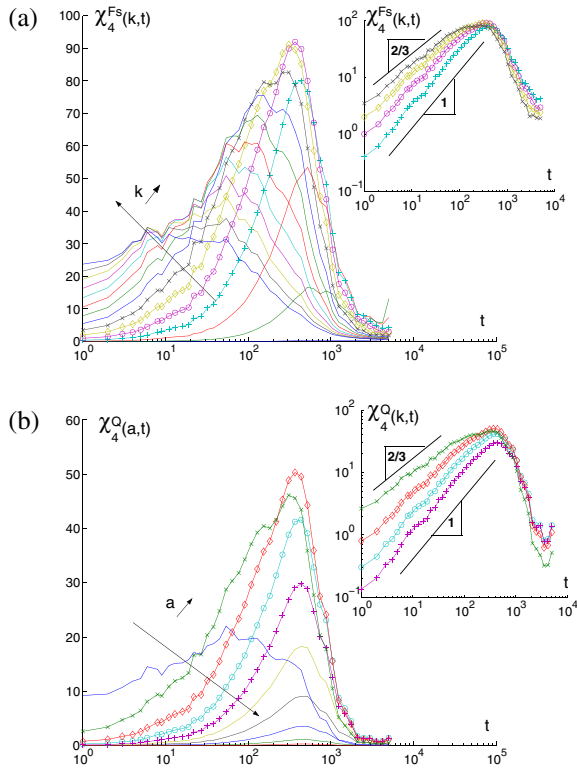


FIG. 3 (color online). (a) $\chi_4^{F_s}(t)$ as a function of time for odd values of $k = 1, 3, \dots, 29$. Inset: Log-Log plot for $k = 7, 9, 11, 13$. (b) $\chi_4^Q(t)$ as a function of time for values of $a = 0.05, 0.1, \dots, 0.5$. Inset: Log-Log plot for $a = 0.1, 0.15, 0.2, 0.25$.

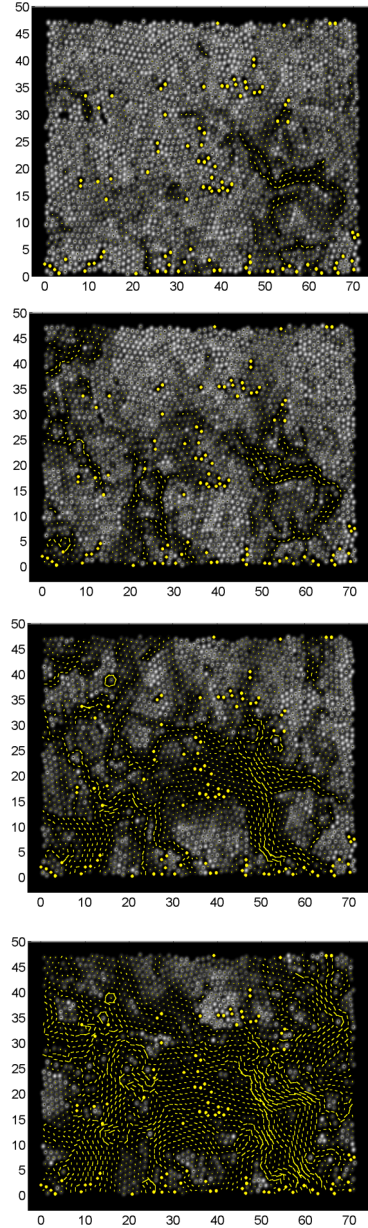


FIG. 4 (color online). Grey-scale plot of $\hat{q}_s^a(r, t)$, at $t = 42, 435, 1113, 2526$ from top to bottom ($a = 0.15$). Black regions correspond to lower values of \hat{q}_s^a . The displacements of the particles during the interval of time t are plotted in white (yellow online). The white (yellow online) dots are particles that have been lost during tracking.

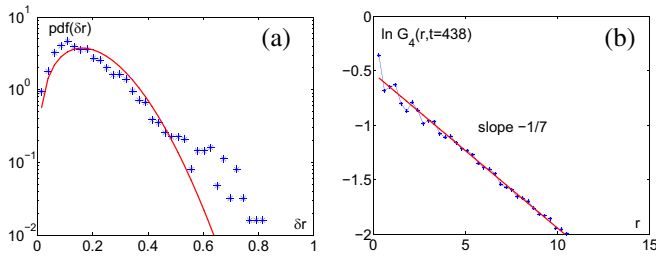


FIG. 5 (color online). (a) self part of the Van Hove correlation function after angular integration at $t = 438$; the solid line is the probability distribution function (pdf) for a Gaussian distribution. (b) $\ln(G_4(r, 438))$ as a function of r (for $a = 0.15$); the straight line is a linear fit.

$t = 0$ moved away more than a in the time interval t then $\hat{q}_s^a(r, t) \approx 0$. The yellow lines in Fig. 4 are the particle displacements in the time interval t . At short-times ($t = 42$) only a few particles have moved and from Fig. 4 it appears that they do so in a stringlike fashion. On larger times ($t = 435, 1113$) the relaxed regions are ramified and finally, at very long time ($t = 2526$) the majority of the particles has moved substantially but there remain few (rather large) regions not yet relaxed. These findings, similar to those found in simulation of supercooled liquids [9–12], suggest that the mobility is organized in clusters, which are the direct visual evidence of the dynamical heterogeneities.

Figure 5(a) displays the probability distribution of the grains displacement for $t = 438$ [corresponding to the maximum of $\chi_4^O(t)$] and quantifies the excess of fast and slow grains compared to the Gaussian distribution (in the solid line). In Fig. 5(b), $G_4(r, 438)$, the radial autocorrelation of q_s^a , averaged over ten realizations (for $a = 0.15$), exhibits an exponential decay over a characteristic dynamical length $\xi = 7$, in agreement with the value obtained from the peak of χ_4^F . For comparison, the dynamic length scales reported in experiments close to the glass transition are of the order of 5–10 molecular diameters [13]. In conclusion, our results, to our knowledge the first extensive experimental study of two and four point *spatiotemporal* dynamic correlation functions, furnish a direct experimental evidence that granular materials close to jamming have an heterogeneous and correlated dynamics. It would certainly be worth studying the possible relations between the dynamic correlations we have found and the diverging length scales that have been proposed to show up at the jamming transition (coming from the jammed phase) [22]. Our results reveal a remarkable similarity with glass-forming liquids that reinforces the connection between glasses and jamming systems [1]. They open the way to further analysis, varying a control parameter (as is the temperature for liquids and packing fraction for colloids), or during compaction. That would give other important information on the microscopic dynamics and provide stringent constraints to the theory of glassy and jammy materials in general.

We thank all the participants in our “Glassy Working Group” in Saclay and, in particular, J.-P. Bouchaud for enriching and enlightening discussions. We thank C. Gasquet and V. Padilla for technical assistance. G. B. is partially supported by the European Community’s Human Potential Programme contracts HPRN-CT-2002-00307 (DYGLAGEMEM).

- [1] A. J. Liu and S. Nagel, *Nature (London)* **396**, 21 (1998).
- [2] G. D’Anna and G. Gremaud, *Nature (London)* **413**, 407 (2001).
- [3] J. B. Knight *et al.*, *Phys. Rev. E* **51**, 3957 (1995); P. Philippe and D. Bideau, *Europhys. Lett.* **60**, 677 (2002).
- [4] C. Josserand, A. V. Tkachenko, D. M. Mueth, and H. Jaeger, *Phys. Rev. Lett.* **85**, 3632 (2000); A. Kabla and G. Debrégeas, *Phys. Rev. Lett.* **92**, 035501 (2004).
- [5] O. Pouliquen, M. Belzons, and M. Nicolas, *Phys. Rev. Lett.* **91**, 014301 (2003).
- [6] G. Marty and O. Dauchot, *Phys. Rev. Lett.* **94**, 015701 (2005).
- [7] E. R. Weeks, J. C. Crocker, A. C. Levitt, A. Schofield, and D. A. Weitz, *Science* **287**, 627 (2000).
- [8] W. Kob and H. C. Andersen, *Phys. Rev. E* **52**, 4134 (1995); *Phys. Rev. E* **51**, 4626 (1995).
- [9] H. C. Andersen, *Proc. Natl. Acad. Sci. U.S.A.* **102**, 6686 (2005).
- [10] M. M. Hurley and P. Harrowell, *Phys. Rev. E* **52**, 1694 (1995).
- [11] N. Lacevic, F. W. Starr, T. B. Schroeder, and S. C. Glotzer, *J. Chem. Phys.* **119**, 7372 (2003), and refs. therein.
- [12] L. Berthier, *Phys. Rev. E* **69**, 020201(R) (2004); S. Whitelam, L. Berthier, and J. P. Garrahan, *Phys. Rev. Lett.* **92**, 185705 (2004).
- [13] M. A. Ediger, *Annu. Rev. Phys. Chem.* **51**, 99 (2000).
- [14] P. Ball, *Nature (London)* **399**, 207 (1999).
- [15] A. Lefèvre, L. Berthier, and R. Stinchcombe, *Phys. Rev. E* **72**, 010301 (2005).
- [16] J. J. Aizenzon, Y. Levin, and M. Sellitto, *Physica (Amsterdam)* **325A**, 371 (2003).
- [17] S. Franz and G. Parisi, *J. Phys. Condens. Matter* **12**, 6335 (2000); C. Donati, S. Franz, S. C. Glotzer, and G. Parisi, *J. Non-Cryst. Solids* **307**, 215 (2002).
- [18] Four point correlation functions, not resolved in space, have already been measured in colloidal systems [A. Duri *et al.*, *Fluctuation Noise Lett.* **5**, L1 (2005)] and in crystalline materials; Mocuta *et al.*, *Science* **308**, 1287 (2005).
- [19] L. F. Cugliandolo and J. L. Iguain, *Phys. Rev. Lett.* **85**, 3448 (2000).
- [20] G. Biroli and J.-P. Bouchaud, *Europhys. Lett.* **67**, 21 (2004).
- [21] C. Toninelli, M. Wyart, L. Berthier, G. Biroli, and J.-P. Bouchaud, *Phys. Rev. E* **71**, 041505 (2005).
- [22] L. E. Silbert, A. J. Liu, and S. R. Nagel, *Phys. Rev. Lett.* **95**, 098301 (2005), and references therein; Matthieu Wyart, Sidney R. Nagel, and T. A. Witten, *Phys. Rev. E* **72**, 051306 (2005).